

Tachyon inflation: tests and comparison with single scalar field inflation

D.A.Steer ^{a1} and F.Vernizzi ^{b2}

a) Laboratoire de Physique Théorique³, Bât. 210, Université Paris XI,
91405 Orsay Cedex, France

and

Fédération de recherche APC, Université Paris VII,
2 place Jussieu - 75251 Paris Cedex 05, France.

b) Institut d'Astrophysique de Paris, GR ϵ CO, FRE 2435-CNRS, 98bis boulevard Arago,
75014 Paris, France

Abstract

We compare the standard single scalar field inflationary predictions with those of an inflationary phase driven by a tachyon field. A slow-roll formalism is defined for tachyon inflation, and we derive the spectra of scalar and tensor perturbations as well as the consistency relations. At lowest order the predictions of standard and tachyon inflation are shown to be the same. Higher order deviations are present and their observational relevance is discussed. We then study some typical inflationary tachyon potentials, discuss their observational consequences and compare them with recent data. All the models predict a negative and very small running of the scalar spectral index, and they consistently lie within the 1σ contour of the data set. However, the regime of blue scalar spectral index and large gravity waves cannot be explored by these models. Finally, a new exact solution of the unperturbed and perturbed coupled gravity and tachyon equations is also presented.

¹steer@th.u-psud.fr

²vernizzi@iap.fr

³Unité Mixte de Recherche du CNRS (UMR 8627).

1 Introduction

The recent WMAP data [1, 2, 3, 4, 5] strongly supports the idea that the early universe underwent a phase of accelerated expansion or inflation [6]. Inflation is becoming the dominant paradigm for the generation of super-horizon fluctuations with a scale-invariant spectrum, which are thought to be the origin of the large scale structures.

One typically considers an inflationary phase driven by the potential or vacuum energy of a scalar field, the inflaton, whose dynamics is determined by the Klein-Gordon action [7]. More recently, however, motivated by string theory, other non-standard scalar field actions have been used in cosmology. In k -inflation [8] higher-order scalar kinetic terms in the action can, without the help of the potential, drive an inflationary evolution. In this context, models of quintessence such as k -essence may also resolve the coincidence problem [9, 10] (see, however, [11]). One particular model of k -inflation which has recently attracted a great deal of attention is tachyon inflation (see e.g. [12]), where the tachyon action is given by

$$S_T = - \int d^4x \sqrt{-g} V(T) (1 + g^{\mu\nu} \partial_\mu T \partial_\nu T)^{1/2} \quad (1.1)$$

and the metric has signature $-, +, +, +$. The tachyon T is a real scalar field with dimensions of length and $V(T)$ is its potential.

The motivations for studying the action Eq. (1.1) come from type II string theory. There the tachyon signals the instability of unstable and uncharged D-branes of tension λ , and different approaches [13] have led to the effective tachyon action being of the Dirac-Born-Infeld form given in Eq. (1.1). In this context the positive potential $V(T)$ is even, has a global maximum at $T = 0$, and minima as $|T| \rightarrow \infty$ where $V \rightarrow 0$. Different potentials have been calculated, but one with particularly attractive properties¹ that will be studied in Section 5 is [18, 19, 20]

$$V(T) = \frac{\lambda}{\cosh(T/T_0)}. \quad (1.2)$$

Numerous papers (see for example [12, 21, 22, 23, 24, 25, 26, 27] and references within) have investigated the cosmological consequences of the gravity-tachyon system,

$$S = \int d^4x \sqrt{-g} \frac{R}{16\pi G} + S_T, \quad (1.3)$$

including slow-roll inflation in the potential $V(T)$. Indeed, many potentials with the properties outlined above can drive inflation, which typically takes place at a scale characterized by the brane tension, $H \sim \lambda^{1/2}/M_{\text{Pl}}$, where $M_{\text{Pl}} = (8\pi G)^{-1/2}$. Furthermore, Sen [28] has pointed out that the rolling tachyon can contribute to the energy density of the universe with dust-like equation of state, $P = 0$. This has raised the question

¹Sen's conjecture [14] is that the static kink-like solutions of the tachyon action are the stable D-brane into which the non-BPS brane decays. For the inverse cosh potential these kinks have special properties [15, 16, 17].

of whether the tachyon could at the same time drive inflation and later behave as dark matter.

As a possible mechanism for driving inflation, tachyon condensation has been criticized in [23, 24]. The main reason is that for string theory motivated values of the parameters in $V(T)$, there is an incompatibility between the slow-roll condition and the COBE normalisation of fluctuations: Inflation generally takes place at an energy scale $\lambda^{1/4}$ with $T \sim T_0$, and in string theory $T_0 \sim 1/M_s$ where M_s is the string mass, and

$$\lambda = \frac{M_s^4}{g_s(2\pi)^3}, \quad (1.4)$$

where g_s is the string coupling. The useful constant dimensionless ratio [22]

$$X_0^2 \equiv \frac{\lambda T_0^2}{M_{\text{Pl}}^2} \quad (1.5)$$

appears in the slow-roll parameters derived from these potentials and typically $X_0 \gg 1$ in order for the slow-roll conditions to be satisfied. One can then see that for natural values of g_s and M_s , slow-roll $X_0^2 \gg 1$ takes only place at an energy scale which is too big to be compatible with the COBE constraint $H/M_{\text{Pl}} \sim \lambda^{1/2}/M_{\text{Pl}}^2 \sim 10^{-5}$. Potentials can, however, be found for which these issues may be circumvented (see also e.g. [29, 30] in the braneworld context).

This criticism has cast a shadow on the string motivation of this scenario but cannot deny the fact that a field satisfying the action Eq. (1.3) with $V(T)$ describing an instability, can naturally lead to inflation. However, as in standard inflation, one needs a small parameter (in this case $(T_0 M_{\text{Pl}})^{-1}$) in order to have a successful inflationary phase.

Thus, despite this criticism and regardless of the string motivations, here we take a phenomenological approach and study the inflationary predictions of a phase of inflation driven by a field T satisfying the action Eq. (1.3). We call this tachyon inflation although the potential $V(T)$ may not be particularly string inspired. However, throughout this paper we assume that $V(T)$ satisfies the properties mentioned above, namely

$$V(0) = \lambda, \quad V'(T > 0) < 0, \quad V(|T| \rightarrow \infty) \rightarrow 0. \quad (1.6)$$

The questions we address here are: 1) Does tachyon inflation lead to the same predictions as standard single field inflation (SSFI)? 2) Can tachyon inflation already be ruled out by current observations? 3) Can we discriminate between tachyon inflation and SSFI in the light of new and planned future experiments?

The answer to the first question is no: tachyon inflation leads to a deviation in one of the second order consistency relations. However, the answer to the second question is that tachyon inflation cannot be ruled out at the moment, and its predictions are typically characteristic of small field or chaotic inflation. The answer to the final question may also be negative: no characteristic signatures of tachyon inflation are likely to be detectable by planned observations but this may change in the future.

Before concluding this section, a comment is in order here. As opposed to action (1.1), the linear action

$$S_T = - \int d^4x \sqrt{-g} V(T) (1 + g^{\mu\nu} \partial_\mu T \partial_\nu T) \quad (1.7)$$

can be put into the standard Klein-Gordon form for a scalar field ϕ : let

$$T = T(\phi) \quad \text{with} \quad d\phi = \sqrt{2V(T)} dT. \quad (1.8)$$

Then the corresponding potential for ϕ is

$$W(\phi) = V(T(\phi)) \quad (1.9)$$

so that the inflationary predictions of action (1.7) are the same as those of SSFI (see the Appendix, Sec. B). When the square root is present a similar change of variables cannot be found, though the square root can be linearized at the expense of introducing an auxiliary field which can either be another scalar field [31] or a metric field [16]. Here we compare tachyon inflation with SSFI, and hence any expansion of action (1.1) in powers of $\partial_\mu T \partial^\mu T$ must go beyond the first order term in order for differences to be found.

This paper is set up in the following way. In Section 2 we consider the unperturbed tachyon system coupled to gravity. We present (Section 3) a new exact solution to Eq. (1.3) which shows explicitly the inflationary and dust-like properties of the solution. Slow-roll parameters are derived in Section 4, where we use the definition introduced in [32]. This is the natural one when comparing models in which inflation is driven by different types of fields. The spectra of scalar and tensor perturbations and the running of the spectral indexes are also derived in Section 4. We show that one of the next to lowest order consistency relations is different from the one predicted by SSFI. In Section 5, different potentials $V(T)$ are studied and their predictions compared with recent data. In the Appendix, Sec. B, we review and clarify the large and small scale perturbations of a tachyon fluid. In fact, in order to highlight the differences and similarities between tachyon inflation and SSFI, in the Appendix, Sec. A, we consider the slightly more general action $S = - \int d^4x \sqrt{-g} V(T) (1 + g^{\mu\nu} \partial_\mu T \partial_\nu T)^q$. In the following we often denote

$$x \equiv T/T_0; \quad (1.10)$$

an overdot denotes a derivative with respect to cosmic time t , and a prime a derivative with respect to the tachyon T .

2 Unperturbed tachyon evolution

We begin by reviewing the background properties of a tachyon dominated universe. From (1.3), the energy momentum tensor for the tachyon is given by

$$T_{\mu\nu} = -V(T)g_{\mu\nu} \sqrt{1 + \partial^\alpha T \partial_\alpha T} + \frac{V(T)}{\sqrt{1 + \partial^\alpha T \partial_\alpha T}} \partial_\mu T \partial_\nu T. \quad (2.1)$$

Now split the tachyon field into a homogeneous time dependent contribution, $T(t)$, and a small \mathbf{x} -dependent perturbation, $\delta T(t, \mathbf{x})$, which describes its quantum fluctuations. In this section we summarize the basic equations for $T(t)$.

The tachyon field can be treated as a fluid with

$$T_{\mu\nu} = (\rho + P)u_\mu u_\nu + P g_{\mu\nu}, \quad (2.2)$$

$$u_\mu = \frac{\partial_\mu T}{(-\partial_\alpha T \partial^\alpha T)^{1/2}}, \quad (2.3)$$

where ρ , P and u_μ are the density, pressure and four-velocity of the fluid, respectively. In a homogeneous and isotropic background, with line element $ds^2 = -dt^2 + a(t)^2 d\mathbf{x}^2$,

$$\rho = \frac{V(T)}{(1 - \dot{T}^2)^{1/2}}, \quad (2.4)$$

$$P = -V(T)(1 - \dot{T}^2)^{1/2}, \quad (2.5)$$

so that the Friedmann equation is

$$H^2 = \frac{1}{3M_{\text{Pl}}^2} \frac{V}{(1 - \dot{T}^2)^{1/2}}, \quad (2.6)$$

whilst energy-momentum conservation gives a second order equation for $T(t)$,

$$\frac{\ddot{T}}{1 - \dot{T}^2} + 3H\dot{T} + (\ln V)' = 0. \quad (2.7)$$

For $\dot{T} \ll 1$ (i.e. during inflation, see below), Eq. (2.7) reduces to a Klein-Gordon equation for a homogeneous scalar field with $\ln V$ playing the rôle of the potential.

It will be convenient to define the ratio

$$w \equiv \frac{P}{\rho} = -1 + \dot{T}^2, \quad (2.8)$$

the adiabatic sound speed,

$$c_A^2 \equiv \frac{\dot{P}}{\dot{\rho}} = -w \left(1 + \frac{2}{3} \frac{(\ln V)'}{H\dot{T}} \right), \quad (2.9)$$

and the effective sound speed [43],

$$c_S^2 \equiv \frac{\partial P / \partial \dot{T}^2}{\partial \rho / \partial \dot{T}^2} = -w, \quad (2.10)$$

which takes into account dissipative effects². For adiabatic perturbations the two sound speeds are the same but in general they are different (see Appendix, Sec. A).

We conclude this section with a remark. For a number of potentials, such as the inverse cosh potential, at early times and small T , $\dot{T}^2 \ll 1$ and $w = -1$, whereas at late times and large T , $\dot{T}^2 \rightarrow 1$ and $w = 0$.³ Furthermore, as summarized in the Appendix, as opposed to a Klein-Gordon scalar field, T can cluster on small scales. For these reasons the tachyon has been studied as a potential unified inflation–dark-matter candidate [12, 21, 23, 24]. This proposal, however, runs into some difficulties [24]: for string-theory motivated potentials, it is not clear how to reheat the universe after inflation (see, however, [34]). Note that in the brane world context reheating can occur very efficiently through gravitational particle production [29, 35]. Furthermore, fine tuning is required for the energy density in the tachyon to take the correct value today [26].

²Equivalently $c_S^2 = \partial P / \partial \rho$ with equation of state $P = -V(T)^2 / \rho$.

³For a large class of potentials, including exponentially decaying potentials, this dust-like behaviour is an attractor solution [33].

3 An inflation to dust exact solution

Though it is somewhat outside the main theme of this paper, here we present a new (and potentially useful) exact solution of the coupled tachyon and gravity equations, Eqs. (2.6) and (2.7), which interpolates between the inflationary and dust phases. Though other exact solutions have been presented in the literature [36, 37], their corresponding potentials do not satisfy the properties given in Eq. (1.6) and do not probe both the inflationary and dust phases.

The form of Eq. (2.7) suggests the ansatz

$$\dot{T} = \tanh(t/T_0), \quad (3.1)$$

where T_0 is a constant. (Without loss of generality we consider $T \geq 0$.) Integrating gives

$$\cosh(t/T_0) = e^{T/T_0}, \quad (3.2)$$

where we have taken $T(0) = 0$. From Eqs. (2.6) and (2.7) it follows that $V(t)$ satisfies

$$\frac{\dot{V} \cosh(t/T_0)}{V \sinh(t/T_0)} + \frac{\sqrt{3V}}{M_{\text{Pl}}} \frac{\sinh(t/T_0)}{\sqrt{\cosh(t/T_0)}} = -\frac{1}{T_0}, \quad (3.3)$$

with solution

$$V(t) = \frac{\lambda}{\cosh(t/T_0)} \left[\frac{1}{1 + \frac{\sqrt{3}X_0}{2} (t/T_0 - \tanh(t/T_0))} \right]^2. \quad (3.4)$$

Here we have normalized the potential such that $V(0) = \lambda$ and X_0 is defined in (1.5).

On using Eq. (3.2), $V(T)$ is thus of the form

$$V(T) = \lambda e^{-T/T_0} f(T/T_0, X_0), \quad (3.5)$$

where $f(T)$ is a decreasing function of T . For $T \ll T_0$ (when $t \simeq T_0 \sqrt{2T/T_0}$),

$$f(T/T_0, X_0) \simeq 1 - \sqrt{\frac{8}{3}} X_0 \left(\frac{T}{T_0} \right)^{3/2}, \quad T/T_0 \rightarrow 0, \quad (3.6)$$

whereas for $T \gg T_0$ (when $t \sim T$),

$$f(T/T_0, X_0) \simeq \frac{4}{3X_0^2} \left(\frac{T_0}{T} \right)^2, \quad T/T_0 \rightarrow \infty. \quad (3.7)$$

For small T , $V \simeq \lambda \exp(-T/T_0)$, and the scale of the potential is set by λ . On the other hand, for large T , $V \simeq (M_{\text{Pl}}^2/T_0^2) \exp(-T/T_0) (T_0/T)^2$ and the scale is set by M_{Pl}^2/T_0^2 . For dimensional reasons, this non-perturbative dependence on λ means that V depends explicitly on M_{Pl} .

Finally, combining Eqs. (2.6), (3.2) and (3.4) gives the Hubble parameter

$$H^2 = \frac{X_0^2}{3T_0^2} \left[\frac{1}{1 + \frac{\sqrt{3}X_0}{2} (t/T_0 - \tanh(t/T_0))} \right]^2, \quad (3.8)$$

which is unfortunately not analytically integrable for $a(t)$. However, for large T , where the potential vanishes exponentially and $\dot{T} \rightarrow 1$, it follows from Eq. (3.8) that $H = 2/3t$ and hence that $a \propto t^{2/3}$. Thus again we find the dust-like solution in this limit. For small T when $\dot{T} \rightarrow 0$, $H = \sqrt{\lambda}/\sqrt{3}M_{\text{Pl}}$ and the universe inflates exponentially. Hence this solution interpolates between the two behaviours of the tachyon fluid — the inflationary and dust-like ones. In the remainder of this paper we focus on the inflationary phase.

4 Predictions of tachyon inflation

It is well known that during an inflationary phase, quantum vacuum fluctuations are stretched on scales larger than the horizon. There they are frozen until they reenter the horizon after inflation. Regardless of the field which drives inflation, large scale perturbations with a quasi scale invariant (Harrison-Zel'dovich) spectrum are generated. Deviations from the scale invariance can be measured in terms of the slow-roll parameters which we define in Subsection 4.1. The spectra of scalar and tensor perturbations generated during tachyon inflation are expressed in terms of the slow-roll parameters in Subsection 4.2. We show that at lowest order the spectrum of scalar perturbations is the same as that of SSFI. Next to lowest order corrections are also computed, and they change the consistency relations with respect to those of SSFI (Subsection 4.3). In the next section these results will be applied to particular models of tachyon inflation and compared to recent data.

4.1 Condition for tachyon inflation and slow-roll parameters

For tachyon inflation, the basic condition for accelerated expansion is that

$$\frac{\ddot{a}}{a} = -\frac{1}{6M_{\text{Pl}}^2}(\rho + 3P) = \frac{1}{3M_{\text{Pl}}^2} \frac{V}{(1 - \dot{T}^2)^{1/2}} \left(1 - \frac{3}{2}\dot{T}^2\right) > 0 \quad (4.1)$$

so that $\dot{T}^2 < \frac{2}{3}$. From Eq. (2.7), inflation will last sufficiently long if \ddot{T} is smaller than the friction term due to the expansion,

$$\ddot{T} < 3H\dot{T}. \quad (4.2)$$

Thus as in SSFI, tachyon inflation is based upon the slow evolution of T in its potential $V(T)$, with the slow-roll conditions

$$\ddot{T} \ll 3H\dot{T}, \quad \dot{T}^2 \ll 1, \quad (4.3)$$

so that during inflation

$$\dot{T} \sim -\frac{(\ln V)'}{3H}, \quad H^2 \sim \frac{V}{3M_{\text{Pl}}^2}. \quad (4.4)$$

Now we want to define slow-roll parameters for tachyon inflation. The slow-roll approximation is an expansion in terms of (generally small) quantities derived from appropriate derivatives either of the Hubble parameter H or of the potential $V(T)$. There are

several ways in which to define the Hubble slow-roll parameters for tachyon inflation. Here we use the recently introduced horizon-flow parameters [32] based on derivatives of H with respect to the number of e -foldings N ,

$$N(t) \equiv \int_t^{t_e} H(t) dt, \quad (4.5)$$

where t_e is the end of inflation. Note that for $\dot{T} > 0$

$$dT = -\frac{2}{3} \frac{H'}{H^3} dN. \quad (4.6)$$

These slow-roll parameters are defined as

$$\epsilon_0 \equiv H_*/H, \quad (4.7)$$

$$\epsilon_{i+1} \equiv \frac{d \ln |\epsilon_i|}{dN}, \quad i \geq 0, \quad (4.8)$$

where H_* is the Hubble parameter at some chosen time, and

$$\dot{\epsilon}_i = H \epsilon_i \epsilon_{i+1}. \quad (4.9)$$

Since these definitions are independent of the field driving inflation, they are a natural choice to use in order to compare SSFI and tachyon inflation. They form exactly the same hierarchy of inflationary flow equations as in SSFI (see indeed [38]), though the observables (such as spectral indices) will no longer be related to the ϵ_i in the same way. In terms of T , the definitions (4.7) and (4.8) are

$$\epsilon_1 = \frac{3}{2} \dot{T}^2, \quad (4.10)$$

$$\epsilon_2 = \sqrt{\frac{2}{3\epsilon_1}} \frac{\epsilon'_1}{H} = 2 \frac{\ddot{T}}{H\dot{T}}, \quad (4.11)$$

$$\epsilon_2 \epsilon_3 = \sqrt{\frac{2\epsilon_1}{3}} \frac{\epsilon'_2}{H}. \quad (4.12)$$

(Note that $\sqrt{\epsilon_1} = -\sqrt{\frac{2}{3}}(H'/H^2)$ since $H' = -\frac{3}{2}H^2\dot{T} < 0$.) The first parameter ϵ_1 measures the contribution of \dot{T}^2 to the energy density Eq. (2.4) and, as in SSFI, inflation occurs when $\epsilon_1 < 1$, ending once ϵ_1 exceeds unity. The parameter ϵ_2 measures the ratio of the field acceleration relative to the friction acting on it due to the expansion. The slow-roll conditions, Eq. (4.3), are satisfied when $\epsilon_1, \epsilon_2 \ll 1$.

The Friedmann equation and the conservation equation, Eqs. (2.6) and (2.7), can be rewritten as a Hamilton-Jacobi system,

$$H'^2 - \frac{9}{4}H^4(T) + \frac{1}{4} \frac{1}{M_{\text{Pl}}^4} V^2(T) = 0, \quad (4.13)$$

$$H' = -\frac{3}{2}H^2(T)\dot{T}, \quad (4.14)$$

so that as in SSFI [39], the tachyon inflation solution is an attractor. Note again that only up to first order terms in ϵ_1 is the inflationary dynamics the same as in SSFI. This can be seen by comparing the Friedmann equation for a single scalar field

$$H^2(\phi) \left[1 - \frac{1}{3}\epsilon_1(\phi) \right] = \frac{1}{3M_{\text{Pl}}^2} W(\phi), \quad (4.15)$$

where $W(\phi)$ is the potential of ϕ (see Eq. (1.9), with the one for the tachyon, Eq. (2.6),

$$H^2(T) \left[1 - \frac{2}{3}\epsilon_1(T) \right]^{1/2} = H^2(T) \left[1 - \frac{1}{3}\epsilon_1(T) \right] + \mathcal{O}(\epsilon_1^2) = \frac{1}{3M_{\text{Pl}}^2} V(T). \quad (4.16)$$

On deriving Eq. (4.16) with respect to T , the tachyon potential and its first and second derivatives can be expressed in terms of the slow-roll parameters,

$$\frac{V'}{VH} = -\sqrt{6}\epsilon_1 \left(1 - \frac{2\epsilon_1}{3} + \frac{\epsilon_2}{6} \right) \left(1 - \frac{2\epsilon_1}{3} \right)^{-1}, \quad (4.17)$$

$$\begin{aligned} \frac{V''}{VH^2} &= 3 \left(\epsilon_1 - \frac{\epsilon_2}{2} \right) + \frac{\epsilon_2}{2} \left(5\epsilon_1 - \frac{\epsilon_2}{3} - \epsilon_3 \right) \left(1 - \frac{2}{3}\epsilon_1 \right)^{-1} \\ &+ 6\epsilon_1 \left(1 - \frac{2}{3}\epsilon_1 + \frac{\epsilon_2}{6} \right) \left(1 - \frac{2}{3}\epsilon_1 - \frac{\epsilon_2}{3} \right) \left(1 - \frac{2}{3}\epsilon_1 \right)^{-2}. \end{aligned} \quad (4.18)$$

At second order in the slow-roll parameters, these expressions are different from those of SSFI. At leading order we have⁴

$$\epsilon_1 \simeq \frac{M_{\text{Pl}}^2}{2} \frac{V'^2}{V^3}, \quad (4.19)$$

$$\epsilon_2 \simeq M_{\text{Pl}}^2 \left(-2 \frac{V''}{V^2} + 3 \frac{V'^2}{V^3} \right), \quad (4.20)$$

$$\epsilon_2 \epsilon_3 \simeq M_{\text{Pl}}^4 \left(2 \frac{V'''V'}{V^4} - 10 \frac{V''V'^2}{V^5} + 9 \frac{V'^4}{V^6} \right), \quad (4.21)$$

which should be compared with other definitions given in the literature [22].

In terms of the slow-roll parameters, the number of e -foldings is given by

$$N(T) = \sqrt{\frac{3}{2}} \int_T^{T_e} \frac{H}{\sqrt{\epsilon_1}} dT \simeq \frac{1}{M_{\text{Pl}}^2} \int_{T_e}^T \frac{V^2}{V'} dT. \quad (4.22)$$

Both the slow-roll parameters and the spectra and amplitude of perturbations are functions of T . Let T_* denote the value of T at which a length scale crosses the Hubble radius during inflation, $k = a_* H_*$. Then the definition of the number of e -foldings, Eq. (4.5), gives

$$a_* = a_e \exp(-N_*), \quad k = a_* H_* = a_e H_* \exp(-N_*), \quad (4.23)$$

⁴In SSFI with potential $W(\phi)$ related to $V(T)$ by Eqs. (1.8) and (1.9), one also finds the following equations up to a multiplicative factor of 1/2 (see Appendix, Sec. B).

leading to

$$\frac{d \ln k}{dT} = -\frac{3}{2} \frac{H^3}{H'} (1 - \epsilon_1), \quad (4.24)$$

at $T = T_*$. Finally, following [40], the comoving scale k can be related to $N_* = N(T_*)$ through

$$N_* = 62 - \ln \frac{k}{a_0 H_0} - \ln \frac{10^{16} \text{GeV}}{V(T_*)^{1/4}} + \ln \frac{V(T_*)^{1/4}}{V_e^{1/4}} - \gamma \ln \frac{V_e^{1/4}}{\rho_{reh}^{1/4}}. \quad (4.25)$$

Here we assume that at the end of inflation when $V = V_e$ the universe is reheated by some unknown mechanism, and the energy density of the universe ρ_{reh} is dominated by radiation. Between the end of inflation and the end of the reheating, the scale factor is assumed to evolve approximately as $a(t) \propto t^\gamma$ with $0 < \gamma < 1$. A model independent upper bound has been given for N_* [41]: it is

$$N_* < 62.5 + \ln \left(\frac{0.6}{h} \right), \quad (4.26)$$

on observationally relevant scales, e.g. when the scale $k = 0.002 \text{ Mpc}^{-1}$ was crossing the horizon. More possibilities are discussed in [42] where the authors find

$$N_* = 63.3 + \frac{1}{4} \ln \epsilon_1, \quad (4.27)$$

for instantaneous reheating, but in extreme cases one can even have $N_* \simeq 100$. Since after tachyon inflation the dynamics of the reheating is still unclear, in the following we shall assume a conservative value of $40 \leq N_* \leq 70$. Since a further unknown parameter (i.e. X_0) is present in the analysis of tachyon inflation, increasing the range of values of N_* does not change qualitatively our analysis.

4.2 Calculating the density perturbations

Calculation of the spectra of scalar quantum fluctuations proceeds by defining a canonical variable which can be quantized with the standard methods. The straightforward generalization of the canonical variable to the case of a tachyon fluid is (see [23, 43, 44]),

$$\mathbf{v}_{\mathbf{k}} = z M_{\text{Pl}} \mathcal{R}_{\mathbf{k}}, \quad (4.28)$$

where $\mathcal{R}_{\mathbf{k}}$ is the curvature perturbation defined in the Appendix, Eq. (A.7), and where the pump field z is defined by

$$z = \frac{\sqrt{3} a \dot{T}}{(1 - \dot{T}^2)^{1/2}} = \frac{a \sqrt{2\epsilon_1}}{c_S}. \quad (4.29)$$

The equation derived from minimizing the action expanded to second order in $\mathbf{v}_{\mathbf{k}}$ is [43]

$$\frac{d^2 \mathbf{v}_{\mathbf{k}}}{d\tau^2} + (c_S k^2 - U(\tau)) \mathbf{v}_{\mathbf{k}} = 0, \quad U(\tau) \equiv \frac{1}{z} \frac{d^2 z}{d\tau^2}. \quad (4.30)$$

It is important to note the factor of $c_S = -w$ in front of k^2 . Before computing $U(\tau)$ in terms of the slow-roll parameters, we observe that in SSFI inflation the pump field is [45] (see also the Appendix),

$$z_{\text{SSFI}} \equiv a\sqrt{2\epsilon_1} = z \left(1 - \frac{2}{3}\epsilon_1\right)^{1/2}, \quad (4.31)$$

differing from z by a first order term in ϵ_1 . It follows that

$$\begin{aligned} U &= U_{\text{SSFI}} + \frac{2}{3} \left(\frac{1}{z} \frac{dz}{d\tau} \frac{d\epsilon_1}{d\tau} + \frac{1}{2} \frac{d^2\epsilon_1}{d\tau^2} \right) \left(1 - \frac{2}{3}\epsilon_1\right)^{-1} + \frac{1}{9} \left(\frac{d\epsilon_1}{d\tau} \right)^2 \left(1 - \frac{2}{3}\epsilon_1\right)^{-2} \\ &= U_{\text{SSFI}} + a^2 H^2 \epsilon_1 \epsilon_2 + \mathcal{O}(\epsilon_i^3), \end{aligned} \quad (4.32)$$

where we have used Eq. (4.9) and $dz/d\tau \simeq zaH$ at lowest order. Therefore, up to first order in ϵ_1 and ϵ_2 , the term $U(\tau)$ in Eq. (4.30) is the same as the one appearing in SSFI, $U_{\text{SSFI}}(\tau)$. The correction $\propto \epsilon_1 \epsilon_2$ allows us to compute U up to second order in the slow-roll expansion from U_{SSFI} given in [32]. Alternatively, $U(\tau)$ can be computed directly from the expression,

$$U = 2a^2 H^2 \left\{ 1 + \frac{3}{2} \dot{T}^2 \left(1 + \frac{V'}{HVT} \right) + \frac{V'^2}{H^2 V^2} - \frac{1}{2} \frac{V''}{H^2 V} \right\} \quad (4.33)$$

$$= a^2 H^2 \left(2 - \epsilon_1 + \frac{3}{2} \epsilon_2 + \frac{1}{4} \epsilon_2^2 + \frac{1}{2} \epsilon_1 \epsilon_2 + \frac{1}{2} \epsilon_2 \epsilon_3 \right) + \mathcal{O}(\epsilon_i^3). \quad (4.34)$$

Though U given in Eq. (4.33) can easily be calculated exactly using Eqs. (4.17) and (4.18), we have only written down explicitly the second order expression in (4.34). This is sufficient to derive the spectrum of perturbations and the consistency equations up to second order. As usual, the zeroth order term $2a^2 H^2$ ensures that the spectrum is scale invariant.

Following standard procedures, we look for a solution to Eq. (4.30) by first expressing the conformal time parameter τ as [32]

$$\tau = -\frac{1}{aH(1-\epsilon_1)} + \int \frac{\epsilon_1 \epsilon_2}{(1-\epsilon_1)^2 aH} dN = -\frac{1}{aH} (1 + \epsilon_1) + \mathcal{O}(\epsilon_i^2). \quad (4.35)$$

As given by Eq. (4.9), to first order ϵ_1 is constant and $aH\tau$ can be taken to be constant for each k mode (though not necessarily the same constant for different k). On substituting aH from Eq. (4.35) into the first order expansion Eq. (4.34), Eq. (4.30) becomes

$$\frac{d^2 \mathbf{v}_{\mathbf{k}}}{d\tau^2} + \left(|w| k^2 - \frac{(\nu^2 - 1/4)}{\tau^2} \right) \mathbf{v}_{\mathbf{k}} = 0, \quad (4.36)$$

where

$$\nu \simeq \frac{3}{2} + \epsilon_1 + \frac{1}{2} \epsilon_2. \quad (4.37)$$

The appropriately normalized solution with the correct asymptotic behavior is

$$\mathbf{v}_{\mathbf{k}} \rightarrow \frac{1}{\sqrt{2k_w}} e^{ik_w \tau}, \quad k_w/aH \rightarrow \infty, \quad (4.38)$$

where we have defined $k_w \equiv \sqrt{-w}k$. Hence, up to a phase,

$$v_{\mathbf{k}} = \frac{\sqrt{\pi}}{2}(-\tau)^{1/2}H_{\nu}^{(1)}(-k_w\tau), \quad (4.39)$$

where $H_{\nu}^{(1)}$ is the Hankel function of the first kind of rank ν . Since we are interested in the power spectrum of this solution in the limit where all the modes are well outside the horizon, only the dominant contribution of the asymptotic form of the Hankel functions for $k_w/aH \rightarrow 0$ is considered, yielding

$$\mathcal{P}_{\mathcal{R}}^{1/2}(k) \equiv \sqrt{\frac{k^3}{2\pi^2}}|\mathcal{R}_{\mathbf{k}}| = 2^{\nu} \frac{\Gamma(\nu)}{\Gamma(3/2)}(-w)^{\frac{1-\nu}{2}}(1+\epsilon_1)^{1/2-\nu} \frac{H}{8\pi M_{\text{Pl}}\sqrt{\epsilon_1}} \Big|_{k=aH}. \quad (4.40)$$

This is the asymptotic value of the power spectrum of perturbations for $k_w/aH \rightarrow 0$, written in terms of quantities evaluated at horizon crossing $k = aH$. It corresponds to the result found for k -inflation with $c_s^2 = -w$ (see the Appendix, Sec. B). On expanding in the slow-roll parameters it leads to

$$\begin{aligned} \mathcal{P}_{\mathcal{R}}^{1/2}(k) &= (-w)^{-1/4} \left[1 - (C+1)\epsilon_1 - \frac{1}{2}C\epsilon_2 \right] \frac{H}{2\sqrt{2}\pi M_{\text{Pl}}\sqrt{\epsilon_1}} \Big|_{k=aH} \\ &= \left[1 - (C+1-\alpha)\epsilon_1 - \frac{1}{2}C\epsilon_2 \right] \frac{H}{2\sqrt{2}\pi M_{\text{Pl}}\sqrt{\epsilon_1}} \Big|_{k=aH}, \quad \alpha = \frac{1}{6}, \end{aligned} \quad (4.41)$$

where $C \equiv -2 + \ln 2 + \gamma \simeq -0.72$ is a numerical constant, γ being the Euler constant originating in the expansion of the gamma function. The parameter α vanishes in SSFI. Indeed, Eq. (4.41) gives the same spectrum as that of SSFI except for the factor $(-w)^{-1/4} \simeq (1+\alpha\epsilon_1)$. This factor will lead to a modification of one of the second order consistency equations.

The spectrum of gravity waves in tachyon inflation is exactly as in SSFI since in absence of anisotropic stress gravity waves are decoupled from matter. The first order result is (see e.g., [40]),

$$\mathcal{P}_g^{1/2}(k) = [1 - (1+C)\epsilon_1] \frac{\sqrt{2}}{\pi} \frac{H}{M_{\text{Pl}}} \Big|_{k=aH}. \quad (4.42)$$

4.3 Consistency relations

We now derive the consistency relations [40] linking the tensor-scalar ratio r , the scalar spectral index n , and the tensor spectral index n_T defined by [3],

$$r \equiv \frac{\mathcal{P}_g}{\mathcal{P}_{\mathcal{R}}}, \quad (4.43)$$

$$n \equiv 1 + \frac{d \ln \mathcal{P}_{\mathcal{R}}(k)}{d \ln k}, \quad (4.44)$$

$$n_T \equiv \frac{d \ln \mathcal{P}_g(k)}{d \ln k}. \quad (4.45)$$

The consistency equations are conditions on the observable parameters, and they are thought to be distinctive of SSFI. By finding deviations from the standard consistency conditions we could in principle find a way of distinguishing tachyon inflation from SSFI.

As discussed above, only at next to lowest order does tachyon inflation lead to deviations from SSFI. Indeed, as expected, to lowest order in the slow-roll parameters r , n , and n_T are identical to those of SSFI,

$$r = 16\epsilon_1, \quad (4.46)$$

$$n = 1 - 2\epsilon_1 - \epsilon_2, \quad (4.47)$$

$$n_T = -2\epsilon_1, \quad (4.48)$$

so the lowest order consistency relation is also the same,

$$r = -8n_T. \quad (4.49)$$

Starting from Eqs. (4.41) and (4.42), we can compute n and n_T up to second order in the slow-roll parameters,

$$n - 1 = -2\epsilon_1 - \epsilon_2 - [2\epsilon_1^2 + (2C + 3 - 2\alpha)\epsilon_1\epsilon_2 + C\epsilon_2\epsilon_3], \quad (4.50)$$

$$n_T = -2\epsilon_1 [1 + \epsilon_1 + (1 + C)\epsilon_2]. \quad (4.51)$$

This expression for n_T is of course identical to that of SSFI, whilst n is different since α is nonzero, $\alpha = 1/6$. Also, the higher to lowest order expression for r (see Eq. (4.43)) is given by

$$r = 16\epsilon_1 [1 + C\epsilon_2 - 2\alpha\epsilon_1]. \quad (4.52)$$

The term $-2\alpha\epsilon_1$ is absent in SSFI and distinctive of tachyon inflation. By combining this expression with Eq. (4.51) and the lowest order results Eqs. (4.46) and (4.47) we get

$$n_T = -\frac{1}{8}r \left[1 - \frac{1 - 2\alpha}{16}r + (1 - n) \right]. \quad (4.53)$$

This consistency relation is the next order version of Eq. (4.49), and there is a clear deviation from SSFI which is represented by a nonvanishing α . Note that this deviation does not depend on any free parameter. Similar modifications of the consistency relations have been discussed in k -inflation models [43] where the authors generically find, at lowest order, $r = -8c_S n_T$, which corresponds to our result with $c_S = (-w)^{1/2} \simeq 1$. Here we have derived a next order consistency equation for the tachyon, Eq. (4.53), which is different from the one of SSFI. However, much larger departures can be caused by other mechanisms [40, 46, 47].

Figure 1 shows

$$Y \equiv n_T + \frac{1}{8}r \left[1 - \frac{1}{16}r + (1 - n) \right] = -\frac{\alpha}{64}r^2 \quad (4.54)$$

as a function of r . The equality $Y = 0$ is satisfied in SSFI and the deviation with $\alpha = 1/6$ shown is a signature of tachyon inflation. However, in order to see the deviation predicted

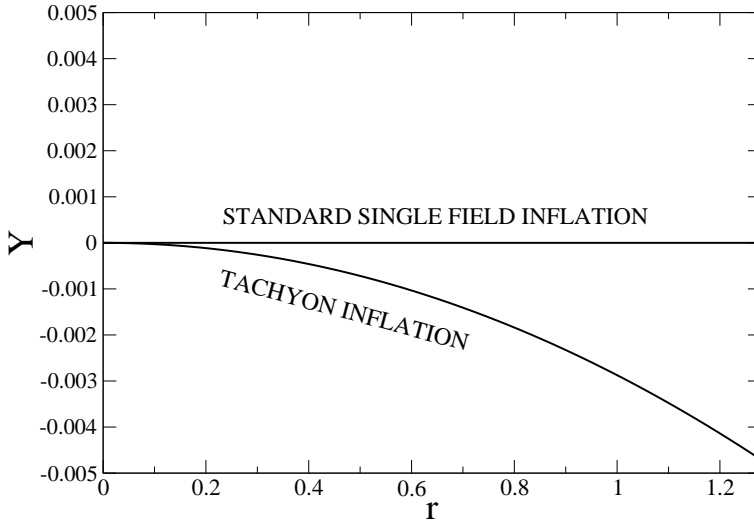


Figure 1: The consistency relation $Y = -\frac{\alpha}{64}r^2$, for SSFI ($\alpha = 0$) and tachyon inflation ($\alpha = 1/6$). In order to be tested, we need n , r , and n_T , with a precision of $\sim 10^{-3}r^2$.

by Eq. (4.53), n , r , and n_T should be known to a precision of $\sim 10^{-3}r^2$. In [46] the error on n_T for future Cosmic Microwave Background observations is estimated. Even for the largest possible values⁵ of r , $r \sim 1$, this is too large for the deviations predicted by the tachyon to be observable, so that Eq. (4.53) will be very difficult to test with planned experiments.

For completeness, we give expressions for the running of the spectral indexes, $dn/d\ln k$ and $dn_T/d\ln k$, which are the same as in SSFI,

$$\frac{dn}{d\ln k} = -2\epsilon_1\epsilon_2 - \epsilon_2\epsilon_3, \quad (4.55)$$

$$\frac{dn_T}{d\ln k} = -2\epsilon_1\epsilon_2. \quad (4.56)$$

From Eq. (4.56) one can derive a third consistency equation, still identical to the SSFI one,

$$\frac{dn_T}{d\ln k} = \frac{1}{8}r \left[\frac{1}{8}r + (n - 1) \right]. \quad (4.57)$$

5 Models of tachyon inflation

We now study tachyon inflation for different potentials $V(T)$ and extract n , n_T , r , and $dn/d\ln k$. We follow the standard procedure [48]: 1) for a given potential compute ϵ_1 , ϵ_2 , and $\epsilon_2\epsilon_3$ as a function of T ; 2) estimate T_e , the value of T at the end of inflation when $\epsilon_1(T_e) = 1$; 3) calculate the number of e -foldings as a function of the field T ; 4) from ϵ_1 ,

⁵As an upper limit on the tensor-scalar ratio we take the 95% upper limit $r < 1.28$ from WMAP with no prior on the spectral index and its running, as quoted in Ref. [3].

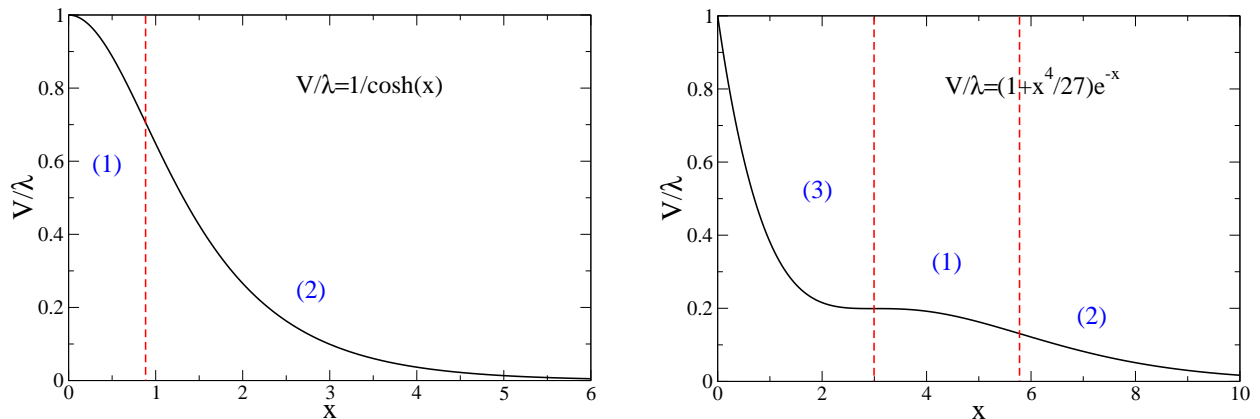


Figure 2: Illustrations of the regimes 1, 2, and 3, for two potentials.

ϵ_2 , and ϵ_3 calculate the observable parameters as a function of T and evaluate them at $T(N_*)$. We consider only $T > 0$.

As in SSFI (see e.g. [7]), we first introduce a general classification scheme for models of tachyon inflation where $V(T)$ satisfies conditions (1.6). In order to classify the available models we distinguish between three possible regimes in which inflation may take place:

1. $V'' \leq 0$, so that $6\epsilon_1 \leq \epsilon_2$,
2. $0 < V'' < V'^2/V$, so that $2\epsilon_1 < \epsilon_2 < 6\epsilon_1$,
3. $V'^2/V \leq V''$, so that $\epsilon_2 \leq 2\epsilon_1$.

Fig. 2 shows these regimes for two potentials studied below. For several aspects and predictions, regime 1 is similar to small field SSFI (although there $V' < 0$ corresponds to $4\epsilon_1 \leq \epsilon_2$). Regime 2 has similarities with large or chaotic SSFI (when $0 < \epsilon_2 < 4\epsilon_1$ in SSFI). Only in regime 3 may n be blue, though we shall see that the “hybrid inflation regime” of SSFI ($n > 1$ and large n_T) cannot be probed.

Note that the parameter X_0 defined in Eq. (1.5) plays a crucial rôle in the classification scheme introduced above, and determines for which values of x inflation occurs. Let $f(x) \equiv V/\lambda$ so that Eqs. (4.19)–(4.20) are just

$$\epsilon_1 = \frac{1}{2X_0^2} \frac{f'^2}{f^3}, \quad (5.1)$$

$$\epsilon_2 = \frac{1}{X_0^2} \left(-2 \frac{f''}{f^2} + 3 \frac{f'^2}{f^3} \right). \quad (5.2)$$

For the potentials we consider, $x_e \equiv T_e/T_0$ increases with X_0 which itself must be sufficiently large that the slow-roll conditions are satisfied, $\epsilon_1, \epsilon_2 \ll 1$, in some range of x . Finally, from Eq. (4.22) the number of e -foldings is

$$N_* = X_0^2 \int_{x_*}^{x_e} \frac{f^2}{|f'|} dx, \quad (5.3)$$

which is a monotonically decreasing function of x_* . Thus for a given N_* (i.e., $N_* \simeq 60$), increasing X_0 also implies increasing of x_* .

Before discussing different examples, note that from the recent limits on the amplitude of scalar and tensor perturbations [3], it is possible to bound λ . At lowest order in ϵ_1 ,

$$\mathcal{P}_{\mathcal{R}} \simeq \frac{V_*}{24\pi^2 M_{\text{Pl}}^4 \epsilon_{1*}} = \frac{2V_*}{3\pi^2 M_{\text{Pl}}^4 r} \simeq 2.95 \times 10^{-9} \times (0.71 + 3 \times 0.01), \quad (5.4)$$

where $0.71 + 3 \times 0.01$ is the 3σ upper limit on the amplitude (at $k = 0.002 \text{ Mpc}^{-1}$). We have

$$V_*^{1/4} \simeq 1.83 \times (r/0.1)^{1/4} \times 10^{16} \text{ GeV}, \quad (5.5)$$

and from the upper bound on gravitational waves $r < 1.28$,

$$\lambda^{1/4} \lesssim 3.46 \times 10^{16} \text{ GeV}. \quad (5.6)$$

For $X_0 \gg 1$ this implies

$$T_0 \gg 2.5 \times 10^4 \ell_{\text{Pl}} \equiv 2.5 \times 10^4 \sqrt{G}. \quad (5.7)$$

5.1 Inverse cosh potential

A number of different tachyon potentials (with the properties mentioned in the introduction) have been derived in the string theory literature. Initially we consider the potential [13, 19]

$$V = \frac{\lambda}{\cosh x}, \quad (5.8)$$

which was studied in a cosmological context in [20]. At first order in the slow-roll approximation, which is valid for $X_0 \gtrsim 3$,

$$\epsilon_1 = \frac{1}{2X_0^2} \frac{\sinh^2 x}{\cosh x}, \quad (5.9)$$

$$\epsilon_2 = \frac{1}{X_0^2} \frac{\cosh^2 x + 1}{\cosh x}, \quad (5.10)$$

$$\epsilon_2 \epsilon_3 = \frac{1}{X_0^4} \frac{\sinh^4 x}{\cosh^2 x}. \quad (5.11)$$

For $x \lesssim 1$, inflation takes place in the regime 1 of our classification, while for $x \gtrsim 1$, it takes place in the regime 2 (see Fig. 2). Inflation ends in regime 2 when $x_e \simeq \ln(4X_0^2) \gtrsim 4$. The spectrum of scalar and tensor perturbations are both red, while the running of the scalar spectral index is always negative,

$$n - 1 = -\frac{2}{X_0^2} \cosh x, \quad (5.12)$$

$$\frac{dn}{d \ln k} = -\frac{2}{X_0^4} \sinh^2 x, \quad (5.13)$$

$$r = -8n_T = \frac{8}{X_0^2} \frac{\sinh^2 x}{\cosh x}. \quad (5.14)$$

To compare the predictions for the inverse cosh potential with data, x_* must first be determined. From Eq. (5.3)

$$N_* = X_0^2 \int_{x_*}^{x_e} \frac{1}{\sinh x} dx = X_0^2 \left[\ln \left(\frac{e^{x_*} + 1}{e^{x_*} - 1} \right) - \ln \left(\frac{e^{x_e} + 1}{e^{x_e} - 1} \right) \right], \quad (5.15)$$

so that

$$\tanh(x_*/2) = \exp(-N_*/X_0^2) \tanh(x_e/2) \simeq \exp(-N_*/X_0^2). \quad (5.16)$$

Thus $X_0^2 \sim N_*$ distinguishes between regime 1 and 2. From the last equality of Eq. (5.16) one finds

$$\sinh x_* = [\sinh(N_*/X_0^2)]^{-1}, \quad \cosh x_* = [\tanh(N_*/X_0^2)]^{-1},$$

so that the observables n , $dn/d \ln k$ and r can be reexpressed in terms of N_* ,

$$n - 1 = -\frac{2}{X_0^2} \frac{1}{\tanh(N_*/X_0^2)}, \quad (5.17)$$

$$\frac{dn}{d \ln k} = -\frac{2}{X_0^4} \frac{1}{\sinh^2(N_*/X_0^2)}, \quad (5.18)$$

$$r = -8n_T = \frac{16}{X_0^2} \frac{1}{\sinh(2N_*/X_0^2)}. \quad (5.19)$$

The running of the spectral index is very small in this model: at the 2σ level

$$0 > \frac{dn}{d \ln k} = -(1 - n) \frac{r}{8} \gtrsim -0.002. \quad (5.20)$$

The potential $V = \lambda(1 + x)e^{-x}$ that has been discussed in the string theory literature [49] has very similar properties to this inverse cosh potential.

5.2 Exponential potential

Another potential which has been derived and studied a great deal in the string and tachyon literature (see for instance [25, 50]) is

$$V(x) = \lambda \exp(-x). \quad (5.21)$$

From Eq. (4.22) we find

$$N_* = X_0^2(e^{-x_*} - e^{-x_e}), \quad (5.22)$$

and to first order in the slow-roll approximation

$$\epsilon_1 = \frac{\epsilon_2}{2} = \frac{1}{2X_0^2} e^x, \quad \epsilon_2 \epsilon_3 = \frac{e^{2x}}{X_0^4}, \quad (5.23)$$

so that this potential is on the border of regimes 2 and 3. Inflation ends when $e^{x_e} = 2X_0^2$ and since $x_* \geq 0$ it follows from Eq. (5.22) that $X_0^2 \geq N_* + 1/2 \gtrsim N_*$. This should be contrasted with the case of the inverse cosh potential: there, a sufficient number of e -foldings can be obtained for any value of X_0 .

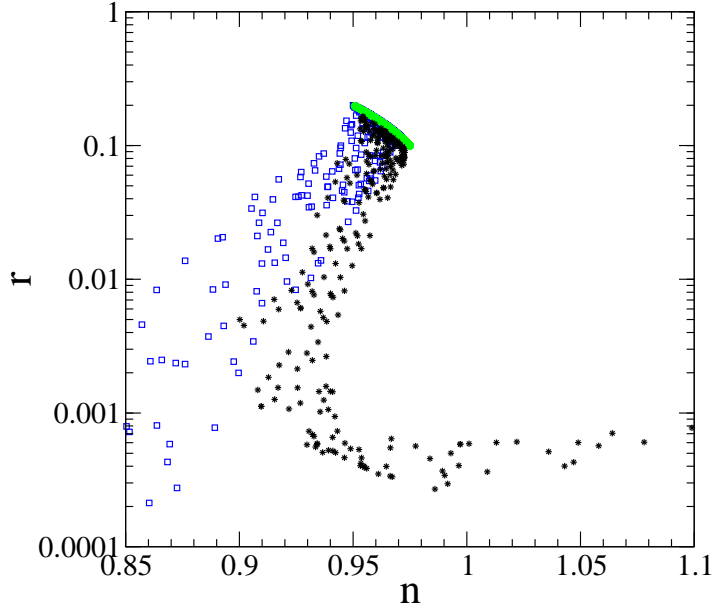


Figure 3: Comparison of the predictions of the inverse cosh potential (squares, blue), the potentials $V = \lambda e^{-x}$ (circle, green), and $V = \lambda(1 + 3^{-3}x^4)e^{-x}$ (stars, black).

The spectrum of scalar and tensor perturbations are both red,

$$n - 1 = -\frac{2}{(N_* + 1/2)}, \quad (5.24)$$

$$\frac{dn}{d \ln k} = -\frac{2}{(N_* + 1/2)^2}, \quad (5.25)$$

$$r = -8n_T = \frac{8}{(N_* + 1/2)}, \quad (5.26)$$

and the running of the spectral index is negative and very small,

$$0 > \frac{dn}{d \ln k} = -\frac{1}{2}(n - 1)^2 = -(1 - n)\frac{r}{8} \gtrsim -0.002 \quad (5.27)$$

at the 2σ level. One should not be surprised that these results are the same as those of chaotic SSFI with $W(\phi) = \frac{1}{2}m^2\phi^2$: when using the change of variables Eq. (1.8) for the linearized action this potential indeed corresponds to $V = \lambda \exp(-x)$. Note also that in the limit $x \rightarrow \infty$ the inverse cosh potential reduces to this exponential potential: as expected, Eqs. (5.17)–(5.19) indeed coincide with Eqs. (5.24)–(5.26) in the $X_0 \rightarrow \infty$ limit. Fig. 3 shows a random sampling of the (n, r) -plane predictions for the inverse cosh potential and $V = \lambda \exp(-x)$. We have varied both X_0 and the number of e -foldings N_* with $40 \leq N_* \leq 70$.

5.3 Inverse power-law potential

In the remainder of this section we no longer work with tachyon potentials derived in string theory. Instead we introduce two phenomenological potentials which still satisfy the properties mentioned in the introduction. The reason for doing this is that they probe region 3 of our classification.

The first potential is an inverse power-law potential such as

$$V = \frac{\lambda}{(1+x^4)}. \quad (5.28)$$

Note that a similar inverse power-law potential, $V \propto 1/x^\alpha$, with $\alpha > 0$, has been considered in [16, 51]. At first order in the slow-roll approximation, which is valid for $X_0 \gtrsim 7$,

$$\epsilon_1 = \frac{8x^6}{X_0^2(1+x^4)}, \quad (5.29)$$

$$\epsilon_2 = \frac{8x^2(x^4+3)}{X_0^2(1+x^4)}, \quad (5.30)$$

$$\epsilon_2\epsilon_3 = \frac{64x^4(x^8+3)}{X_0^4(1+x^4)^2}. \quad (5.31)$$

As opposed to all the potential studied above, when x is large ($x > 3^{1/4}$) inflation occurs in regime 3 of our classification where we expect an important contribution of gravity waves. However, the scalar spectral index is red since $-\epsilon_2 < 2\epsilon_1$ for all x . To leading order in $1/X_0$, inflation ends when

$$x_e^2 = \frac{X_0^2}{8} + \mathcal{O}(X_0^{-2}), \quad (5.32)$$

and from Eq. (5.3) the number of e -foldings is

$$N_* = \frac{X_0^2}{8} \left(\frac{1}{x_*^2} - \frac{1}{x_e^2} \right), \quad (5.33)$$

so that

$$x_*^2 = \frac{X_0^2}{8(1+N_*)} [1 + \mathcal{O}(X_0^{-2})]. \quad (5.34)$$

The spectral indices are red and the running is negative,

$$n-1 = -\frac{24x_*^2}{X_0^2} = -\frac{3}{1+N_*} [1 + \mathcal{O}(X_0^{-2})], \quad (5.35)$$

$$\frac{dn}{d \ln k} = -\frac{192x_*^4}{X_0^4} = -\frac{3}{(1+N_*)^2} [1 + \mathcal{O}(X_0^{-2})], \quad (5.36)$$

$$r = -8n_T = \frac{128x_*^6}{X_0^2(1+x^4)} = \frac{16}{1+N_*} [1 + \mathcal{O}(X_0^{-2})]. \quad (5.37)$$

As for the potentials considered previously, the running of n is very small

$$\frac{dn}{d \ln k} = -\frac{1}{3}(n-1)^2 \gtrsim -0.002, \quad (5.38)$$

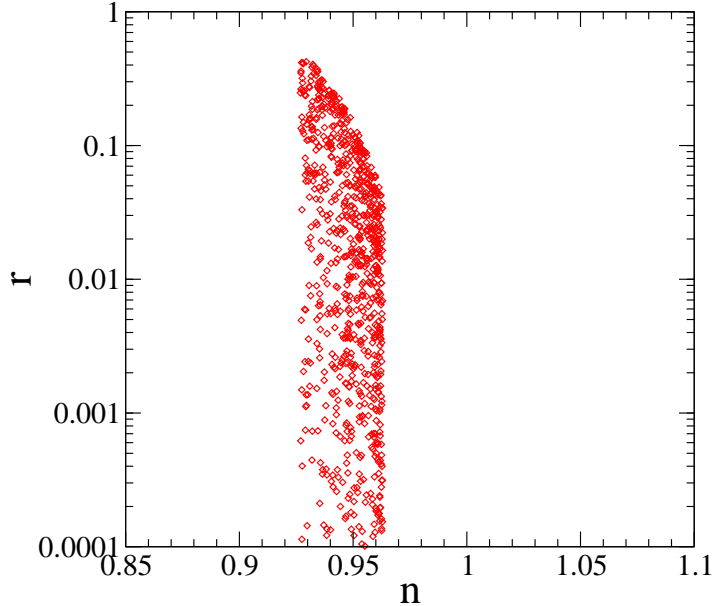


Figure 4: The (n, r) -plane for the inverse power-law potential.

at the 2σ level. Fig. 4 plots a random sampling of the (n, r) -plane for $40 \leq N_* \leq 70$ showing the more important contribution of gravity waves relative to the inverse cosh and exponential potentials.

5.4 Potentials giving $n \geq 1$

All the potentials considered above give $n < 1$. It is legitimate to ask if potentials satisfying the conditions (1.6) can give $n \geq 1$. This requires

$$-\epsilon_2 \geq 2\epsilon_1, \quad (5.39)$$

and the equality is satisfied for $V = \lambda/(1+x)$. More generally the power-law potentials

$$V = \frac{\lambda}{1+x^p} \quad (5.40)$$

with $p \leq 1$ give $n \geq 1$. However, in the absence of other physics, inflation never ends for these potentials since ϵ_1 is a decreasing function of x . In the class of exponential potentials

$$V = \lambda e^{-x^p}, \quad (5.41)$$

the condition Eq. (5.39) requires $p \leq 1$, and $n \geq 1$ when $x_* \leq x_c = [(1-p)/p]^{1/p}$. Once again, other physics such as the coupling to another field is required to end inflation, similarly to hybrid models.

If we remain with models in which inflation ends naturally we can modify V to obtain $n \geq 1$. An example is the potential

$$V = \lambda (1 + (p-1)^{(1-p)} x^p) e^{-x}, \quad (5.42)$$

which is not string theory inspired. For $p = 1$ the predictions are very similar to those of the inverse cosh potential. For $p > 1$ the potential explores regime 3 of our classification (see Fig. 2). By construction, when $x = p - 1$, $V' = V'' = 0$ so that $\epsilon_i = 0$ leading to $n = 1$ and $r = 0$. However, for $x_* \leq p - 1$ we are in regime 3, $n \geq 1$ and $r \propto \epsilon_1$ is very small. Hence, as is confirmed in Fig. 3, this potential leads to a blue scalar spectral index with very small r . This regime is probed by small X_0 . For large X_0 the predictions are the same as the inverse cosh potential (again see Fig. 3).

6 Discussion and conclusion

In the previous section we have described the inflationary predictions of several tachyon potentials. They generally have a red spectrum of scalar perturbations with a negative and very small running of the scalar spectral index. For specific choices of potential such as that given in Eq. (5.42), blue spectra can be obtained with very small r . It is interesting to compare these predictions with the current data and to see whether it is possible to discriminate between SSFI and tachyon inflation.

Since there is a very small running, it is legitimate to ask how well motivated it is to introduce this new higher-order parameter (and hence ϵ_3) when comparing our models with data. Motivated by the discussion of Leach and Liddle [52], we neglect ϵ_3 and use their likelihood analysis to constrain the first two parameters ϵ_1 and ϵ_2 . We consider the same four potentials as in figures 3 and 4 and compare their (n, r) -plane predictions with the 2-dimensional likelihood contours (at 1σ and 2σ). Results are shown in Fig. 5.

For the inverse cosh potential (squares, blue) inflation can take place in both regimes 1 and 2. For a large set of parameters N_* and X_0 (excluding very small X_0), the predictions are well inside the 2σ contour. There are non negligible gravity waves for large X_0 , though for the range of N_* given above, $r \lesssim 0.2$. When $X_0 \rightarrow \infty$, the predictions concentrate on the line $\epsilon_2 = 2\epsilon_1$ which are just those of the exponential potential $V = \lambda e^{-x}$ (circles, black). The inverse power-law potential (diamonds, red) can occupy regimes 1, 2, and 3, and leads to a large contribution of gravity waves, although $r \lesssim 0.2$ in the region not excluded by current data. The potential $V = \lambda(1+x^4/27)e^{-x}$ (stars, black) occupies much of the region of the inverse cosh potential as well as yielding blue spectra for negligible r .

All the presented models seem to be consistent with the data. Hence, the first-year WMAP results are still too crude to constraint significantly the region of parameters. On the other hand, we still lack of information about the mechanism of reheating that could take place after tachyon inflation, leaving us with a large uncertainty on N_* . Progress can be made by better estimating this particular parameter.

Our results point to the fact that it is difficult to distinguish between a model where inflation is driven by a Klein-Gordon scalar field or by some other field satisfying a non standard action. However, none of the potentials we have considered in our analysis, which are those where inflation ends naturally, lead to both a blue scalar spectral index and large gravity wave spectrum. Therefore for these potentials a large region in the (n, r) -plane is not probed by tachyon inflation. This corresponds, in SSFI, to the region occupied by hybrid inflation. Detection of $n > 1$ and large r , or of a large running of n , can lead to the exclusion of tachyonic inflation.

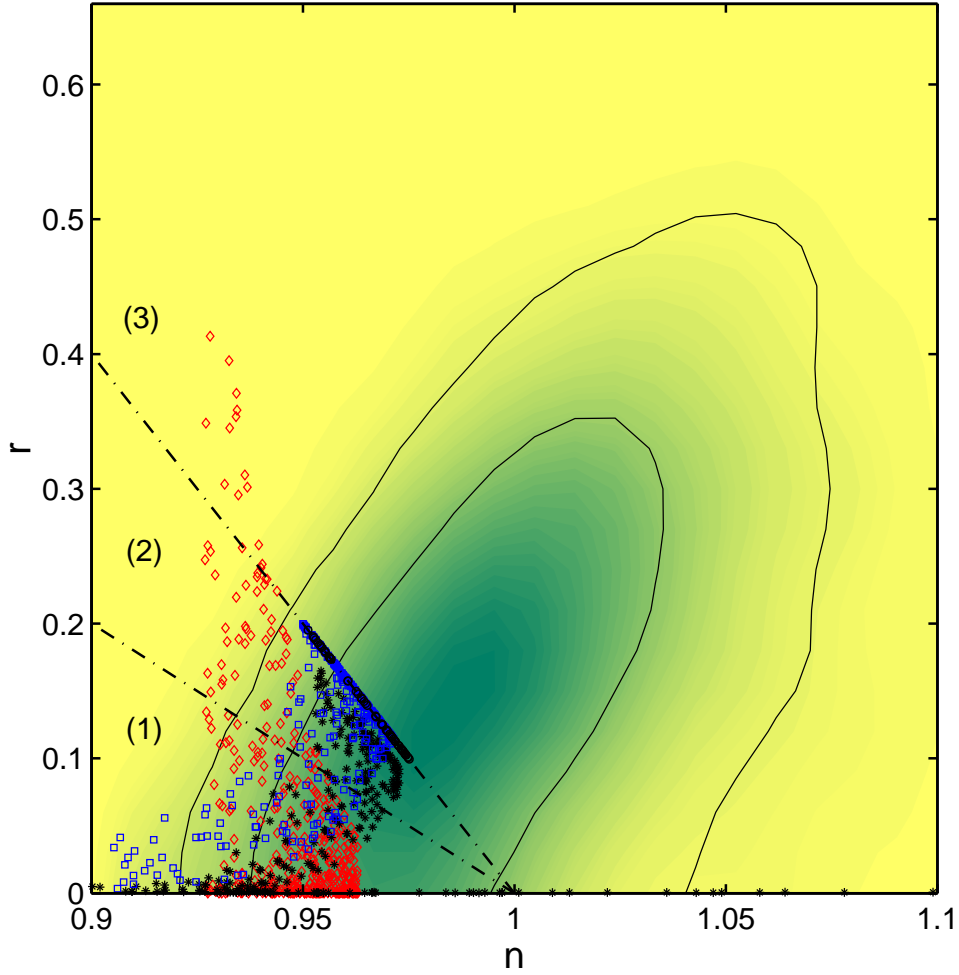


Figure 5: Models of tachyon inflation compared to the 2-dimensional likelihood contours (at 1σ and 2σ) on the (n, r) -plane. The points represent the result of a random sampling from three different tachyonic potentials: inverse cosh potential (squares, blue), $V = \lambda e^{-x}$ (circles, black), the potential $V = \lambda(1 + x^4/27)e^{-x}$ (stars, black), and inverse power-law potential (diamonds, red). The two dashed lines correspond to the limits between the three different regimes of inflation. The likelihood contour comes from the analysis of S. Leach and A. Liddle [52].

In this paper we have discussed tachyon inflation using a phenomenological approach. We have presented a new exact solution of the tachyon-gravity equations which smoothly interpolates between the inflationary and the dust-like regime, and have shown that one of the consistency relations differs from that of standard inflation. It will be difficult to use this equation to discriminate between standard inflation and tachyon inflation with planned observations, but things may improve in the future. However, this modified consistency relation may be useful to constraint other k -type inflationary models as we have discussed in the Appendix. Finally we compared the predictions of tachyon inflation with current data. None of the models presented here can be excluded by the data. We conclude that if the future data point towards small and chaotic single field inflation, it may be difficult to discriminate between tachyon inflation and standard single field inflation, unless other distinguishing criteria appear.

Acknowledgments

It is a pleasure to thank R. Durrer, S. Leach, J. Martin, and R. Rivers for useful discussions and comments, and T. Evans for help with Maple. We acknowledge S. Leach and H. Peiris for providing us with their Markov Chain analyses.

A Tachyon perturbations

In this appendix we recall two important properties of a tachyon dominated universe. First, as for a single standard scalar field dominated universe, the perturbations produced during tachyon inflation are adiabatic. The entropy perturbation is present but it is negligible on large scales, $k/(aH) \rightarrow 0$. This ensures that the large scale perturbations produced during a tachyon inflationary phase are adiabatic, as in SSFI. However, the analogy with the Klein-Gordon scalar field stops here: in contrast to the scalar field, the tachyon can cluster on small scales when $\dot{T}^2 \rightarrow 1$, as was shown in [23, 26] (see also [43] for the same derivation in the context of k -inflation). Here we rederive this result making use of a gauge invariant formalism, and show that the result relies on the fact that the tachyon and the scalar field have different entropy perturbations on small scales.

We study perturbations about the homogeneous solution $T(t)$, considering the coupled system of tachyon and metric perturbations. The perturbed metric is defined by

$$ds^2 = -(1 + 2A)dt^2 + 2a\partial_i B dx^i dt + a^2[(1 - 2\psi)\delta_{ij} + 2\partial_i \partial_j E] dx^i dx^j. \quad (\text{A.1})$$

As in the case of a scalar field, the tachyon has no anisotropic stress and perturbations can be described by two independent variables (e.g. δT and ψ in longitudinal gauge). We now derive evolution equations of the density contrast.

It is convenient to treat the tachyon as a perturbed non adiabatic fluid. Thus, we can define the intrinsic entropy perturbation as [53]

$$\Gamma \equiv \frac{\delta P}{P} - \frac{c_A^2}{w} \frac{\delta \rho}{\rho}. \quad (\text{A.2})$$

For the tachyon

$$P\Gamma = \frac{2}{3} \frac{(\ln V)'}{H\dot{T}} \rho \Delta = (c_S^2 - c_A^2) \rho \Delta, \quad (\text{A.3})$$

where, using the notation of [53], Δ is the gauge invariant density perturbation on the comoving hypersurface relative to the tachyon fluid,

$$\Delta \equiv \frac{\delta\rho}{\rho} + 3H\dot{T}\delta T. \quad (\text{A.4})$$

The last equality of Eq. (A.3) is valid, in general, for any k -field [43].

In the fluid formalism, we find a second order differential equation for Δ [53],

$$\frac{d^2\Delta}{d\tau^2} - \mathcal{H}[3(2w - c_A^2) - 1] \frac{d\Delta}{d\tau} + 3\mathcal{H}^2 \left(\frac{3}{2}w^2 - 4w - \frac{1}{2} + 3c_A^2 \right) \Delta + c_A^2 k^2 \Delta = -wk^2\Gamma, \quad (\text{A.5})$$

where τ is conformal time, $d\tau \equiv dt/a$, and $\mathcal{H} \equiv (da/d\tau)/a$. By using Eq. (A.3) we obtain the evolution equation for the density contrast of a tachyon fluid,

$$\frac{d^2\Delta}{d\tau^2} - \mathcal{H}[3(2w - c_A^2) - 1] \frac{d\Delta}{d\tau} + 3\mathcal{H}^2 \left(\frac{3}{2}w^2 - 4w - \frac{1}{2} + 3c_A^2 \right) \Delta + c_S^2 k^2 \Delta = 0. \quad (\text{A.6})$$

Here the sound horizon $c_S/(aH)$, from the Laplacian term of Eq. (A.6), should be contrasted with $c_A/(aH)$ in the case of an adiabatic fluid where $\Gamma = 0$. The difference is due to the non-zero entropy perturbation Γ which, in the fluid formalism of Eq. (A.5), acts as a source for the evolution equation for the energy density perturbation.

For a standard scalar field $c_S^2 = 1$ while for the tachyon $c_S^2 = -w$. On large scales, when $k/(aH) \rightarrow 0$, Eq. (A.5) is the same for the two fields. In particular, as for a standard scalar field, in a tachyon dominated universe curvature perturbations are conserved and are not affected by entropy perturbations. The curvature perturbation on the comoving hypersurfaces is defined by

$$\mathcal{R} = \psi + H \frac{\delta T}{\dot{T}}. \quad (\text{A.7})$$

On large scales this is sourced only by the entropy perturbation according to [54]

$$\dot{\mathcal{R}} \simeq -3H^2 \frac{P}{\dot{\rho}} \Gamma. \quad (\text{A.8})$$

However, combination of the perturbed energy and momentum constraint equations gives

$$\frac{k^2}{a^2} \Psi = -4\pi G \rho \Delta, \quad (\text{A.9})$$

where Ψ is the Bardeen potential $\Psi = \psi - \mathcal{H}(B - a\dot{E})$. Using Eq. (A.3), the entropy in a tachyon dominated universe becomes

$$P\Gamma = \frac{w + c_A^2 k^2}{4\pi G a^2} \Psi \simeq 0, \quad \text{for } k/(aH) \rightarrow 0, \quad (\text{A.10})$$

and the curvature perturbation \mathcal{R} is conserved on large scales.

However, different c_S^2 's imply a different clustering behaviour on small scales, where the Laplacian term becomes important. It is well known that a standard scalar field (such as quintessence) cannot cluster on length scales smaller than H^{-1} , its Jeans length being of the order $L_J \sim c_S/(aH) = (aH)^{-1}$. For tachyon matter, however, $c_S^2 = -w$ and the effective Jeans length for scalar perturbations is only of order $L_J = (aH)^{-1}(1 - \dot{T}^2)^{1/2}$, which can be very small. Thus the tachyon can cluster on small scales when $\dot{T} \rightarrow 1$.

B Generalized action

Here we consider the action

$$S_T = - \int d^4x \sqrt{-g} V(T) (1 + g^{\mu\nu} \partial_\mu T \partial_\nu T)^q, \quad (\text{B.1})$$

with the aim of clarifying the origin of the differences between tachyon inflation $q = 1/2$ and SSFI $q = 1$.

From Eq. (B.1) it follows that

$$P = -V(1 - \dot{T}^2)^q, \quad (\text{B.2})$$

$$\rho = V(1 - \dot{T}^2)^{q-1} [1 - \dot{T}^2(1 - 2q)], \quad (\text{B.3})$$

$$w = -\frac{(1 - \dot{T}^2)}{1 - \dot{T}^2(1 - 2q)}, \quad (\text{B.4})$$

and the equation of motion for T is

$$(2q) \frac{\ddot{T}}{1 - \dot{T}^2} + 3(2q)H \frac{\dot{T}}{1 - \dot{T}^2(1 - 2q)} + (\ln V)' = 0. \quad (\text{B.5})$$

Inflation ends when

$$\dot{T}^2 = \frac{1}{q+1}. \quad (\text{B.6})$$

The evolution equation for density perturbations about this homogeneous and isotropic background is given by Eq. (A.6) where

$$c_S^2 = 1 + (q-1) \frac{2\dot{T}^2}{1 + \dot{T}^2(1 - 2q)} = 1 + (q-1) \frac{2(1+w)}{1 + (1 - 2q)(2w+1)}. \quad (\text{B.7})$$

For $q = 1/2$, $c_S^2 = -w$; and for $q = 1$, $c_S^2 = 1$ as discussed after Eq. (A.6).

It is straightforward to calculate the number of e -foldings and the slow-roll parameters. From the Friedmann equation with energy density ρ given in Eq. (B.3) it follows that

$$dN = -\frac{3}{2} \frac{H^3}{H'} \left[\frac{2q}{1 - \dot{T}^2(1 - 2q)} \right] dT, \quad (\text{B.8})$$

so that by definition (see Eq. (4.8)),

$$\epsilon_1 \equiv \frac{1}{H} \frac{dH}{dN} = \frac{3}{2} \left[\frac{2q\dot{T}^2}{1 - \dot{T}^2(1 - 2q)} \right]. \quad (\text{B.9})$$

Thus to leading order

$$\epsilon_1 \simeq \frac{1}{2q} \frac{M_{\text{Pl}}^2 V'^2}{V^3}. \quad (\text{B.10})$$

In the calculation of density perturbations, the pump field is now [43]

$$z \equiv \frac{a(\rho + P)^{1/2}}{c_S H} = \sqrt{3} a \sqrt{2q} \dot{T} \left[\frac{1 + \dot{T}^2(1 - 2q)}{(1 - \dot{T}^2)(1 - \dot{T}^2(1 - 2q))} \right]^{1/2} \quad (\text{B.11})$$

$$= a\sqrt{2\epsilon_1} \left(1 - \frac{2}{3}\epsilon_1\right)^{-1/2} \left[1 + \frac{4}{3} \frac{\epsilon_1}{2q}(1 - 2q)\right]^{1/2}. \quad (\text{B.12})$$

For $q = 1$, Eqs. (B.11) and (B.12) correctly reduce to

$$z_{\text{SSFI}} = \frac{\sqrt{6} a \dot{T}}{\sqrt{1 + \dot{T}^2}} = \frac{a \dot{\phi}}{M_{\text{Pl}} H} = a\sqrt{2\epsilon_1}, \quad (\text{B.13})$$

where the second equality is obtained using Eqs (1.8) and (1.9). Thus

$$z_{\text{SSFI}} = z \left(1 - \frac{2}{3}\epsilon_1\right)^{1/2} \left[1 + \frac{4}{3} \frac{\epsilon_1}{2q}(1 - 2q)\right]^{-1/2}, \quad (\text{B.14})$$

which is the generalisation of Eq. (4.31). On differentiation and using Eq. (B.9) we find

$$U = U_{\text{SSFI}} + a^2 H^2 \epsilon_1 \epsilon_2 \left(\frac{1 - q}{q}\right) + \mathcal{O}(\epsilon_i^2), \quad (\text{B.15})$$

again showing clearly the $q = 1$ limit.

The expression for $\mathcal{P}_{\mathcal{R}}(k)$ is exactly as given in Eq. (4.41) but with w replaced by $-c_S^2$ which, to leading order, is given by

$$c_S^2 = 1 - \frac{2(q - 1)}{3q} \epsilon_1 + \mathcal{O}(\epsilon_1^2). \quad (\text{B.16})$$

A straightforward calculation then shows that the general expression for α introduced in Eq. (4.41) is

$$\alpha = \frac{1 - q}{6q}, \quad (\text{B.17})$$

so that $\alpha = 0$ in SSFI and $\alpha = 1/6$ in tachyon inflation. Thus the consistency relations given in Section 4.3 remain valid as a function of q provided the slow-roll expansion holds. The consistency relation

$$n_T + \frac{r}{8} \left[1 - \frac{r}{16} + (1 - n)\right] \equiv Y = -\frac{\alpha r^2}{64} \quad (\text{B.18})$$

can constrain α , and hence q , for large r . For example, when $r \simeq 1$ the error on Y is predicted to be of the order of ~ 0.007 [46]. In that case values of $\alpha \gtrsim 1/2$ corresponding to $q \lesssim 1/4$ could be tested. However, we stress that only $q = 1/2, 1$ are physically relevant values here.

For a given potential $V(T)$, the inflationary predictions of Section 5 depend on q . From Eq. (B.10) this q dependence can simply be obtained by replacing $\epsilon_i \rightarrow \epsilon_i = \epsilon_i/(2q)$ in the calculations of that section. (This factor of $1/(2q)$ originates from action Eq. (B.1): when expanded to first order in \dot{T}^2 its kinetic term differs by a factor of $1/(2q)$ from kinetic term the SSFI action, Eq. (1.7).) For example, consider the exponential potential $V = \lambda \exp(-x)$ of section 5.2. The number of e -foldings is now

$$N_* = \sqrt{2q}X_0^2(e^{-x_*} - e^{-x_e}), \quad (\text{B.19})$$

and to first order in the slow-roll approximation

$$\epsilon_1 = \frac{\epsilon_2}{2} = \frac{1}{[(2q)X_0^2]} \frac{e^x}{2}, \quad \epsilon_2\epsilon_3 = \frac{e^{2x}}{[(2q)X_0^2]^2}. \quad (\text{B.20})$$

Inflation ends when $e^{x_e} = 2(2q)X_0^2$ and Eq. (B.19) imposes $(2q)X_0^2 \geq (\sqrt{2q}N_* + 1/2)$. The q -dependent spectrum of scalar and tensor perturbations are given by

$$n - 1 = -\frac{2}{(\sqrt{2q}N_* + 1/2)}, \quad (\text{B.21})$$

$$\frac{dn}{d \ln k} = -\frac{2}{(\sqrt{2q}N_* + 1/2)^2}, \quad (\text{B.22})$$

$$r = -8n_T = \frac{8}{(\sqrt{2q}N_* + 1/2)}. \quad (\text{B.23})$$

For this potential and for $N_* \gtrsim 40$, the WMAP data constrains $q \gtrsim 0.16$, at the 2σ level.

References

- [1] C. L. Bennett et al., *Astrophys. J. Suppl.* **148** (2003) 1.
- [2] D. N. Spergel et al., *Astrophys. J. Suppl.* **148** (2003) 175.
- [3] H. V. Peiris et al., *Astrophys. J. Suppl.* **148** (2003) 213.
- [4] E. Komatsu et al., *Astrophys. J. Suppl.* **148** (2003) 213.
- [5] G. Hinshaw et al., *Astrophys. J. Suppl.* **148** (2003) 135.
- [6] A. Guth, *Phys. Rev. D* **23** (1981) 347.
- [7] A. R. Liddle, D. H. Lyth, “Cosmological inflation and large-scale structure”, Cambridge University Press, UK, (2000).
- [8] C. Armendariz-Picon, T. Damour and V. Mukhanov, *Phys. Lett. B* **458** (1999) 209.
- [9] T. Chiba, T. Okabe, and M. Yamaguchi, *Phys. Rev. D* **62** (2000) 023511.
- [10] C. Armendariz-Picon, V. Mukhanov and P. J. Steinhardt, *Phys. Rev. D* **63** (2001) 103510.

- [11] M. Malquarti, E. J. Copeland and A. R. Liddle, Phys. Rev. D **68** (2003) 023512.
- [12] G. Gibbons, Phys. Lett. B **537** (2002) 1-4.
- [13] A. Sen, JHEP **9910** (1999) 008; M. R. Garousi, Nucl. Phys. B **584** (2000) 284; M. R. Garousi, Nucl. Phys. B **647** (2002) 117; E. A. Bergshoeff, M. de Roo, T. C. de Wit, E. Eyras and S. Panda, JHEP **0005** (2000) 009; J. Kluson, Phys. Rev. D **62** (2000) 126003; A. Sen, Mod. Phys. Lett. A **17** (2002) 1797; A. Sen, “Time and tachyon,” [arXiv:hep-th/0209122]; D. Kutasov and V. Niarchos, Nucl. Phys. B **66** (2003) 56-70; K. Okuyama, JHEP **0305** (2003) 005; M. R. Garousi, JHEP **0304** (2003) 027.
- [14] A. Sen, JHEP **9809** (1998) 023. JHEP **9812** (1998) 021.
- [15] C. j. Kim, Y. b. Kim and C. O. Lee, JHEP **0305** (2003) 020; C. Kim, Y. Kim, O. K. Kwon and C. O. Lee, “Tachyon kinks on unstable Dp-branes,” [arXiv:hep-th/0305092].
- [16] P. Brax, J. Mourad and D. A. Steer, “Tachyon kinks on non BPS D-branes,” to appear in PLB, [arXiv:hep-th/0304197].
- [17] A. Sen, “Open and closed strings from unstable D-branes,” [arXiv:hep-th/0305011].
- [18] F. Leblond and A. W. Peet, JHEP **0304** (2003) 048.
- [19] N. Lambert, H. Liu and J. Maldacena, “Closed strings from decaying D-branes,” [arXiv:hep-th/0303139].
- [20] C. j. Kim, H. B. Kim, Y. b. Kim and O. K. Kwon, JHEP **0303** (2003) 008.
- [21] G. Gibbons, Class. Quant. Grav. **20** (2003) S321-S346.
- [22] M. Fairbairn and M. H. Tytgat, Phys. Lett. B **546** (2002) 1.
- [23] A. V. Frolov, L. Kofman and A. A. Starobinsky, Phys. Lett. B **545** (2002) 8.
- [24] L. Kofman and A. Linde, JHEP **0207** (2002) 004.
- [25] M. Sami, P. Chingangbam and T. Qureshi, Phys. Rev. D **66** (2002) 043530.
- [26] G. Shiu and I. Wasserman, Phys. Lett. B **541** (2002) 6-15.
- [27] T. Padmanabhan and T. Roy Choudhury, Phys. Rev. D **66** (2002) 081301.
- [28] A. Sen, JHEP **0204** (2002) 048; A. Sen, JHEP **0207** (2002) 065.
- [29] M. C. Bento, O. Bertolami and A. A. Sen, Phys. Rev. D **67** (2003) 063511; M. C. Bento, N. M. C. Santos, A. A. Sen, [arXiv:astro-ph/0307292].
- [30] S. Mukohyama, Phys. Rev. D **66** (2002) 024009.

- [31] M. Malquarti, E. J. Copeland, A. R. Liddle and M. Trodden, Phys. Rev. D **67** (2003) 123503.
- [32] D. J. Schwarz, C. A. Terrero-Escalante, A. A. Garcia, Phys. Lett. B **517** (2001) 243.
- [33] T. Mehen and B. Wecht, JHEP **0302** (2003) 058.
- [34] J. M. Cline, H. Firouzjahi and P. Martineau, JHEP **0211** (2002) 041.
- [35] E. J. Copeland, A. R. Liddle and J. E. Lidsey, Phys. Rev. D **64** (2001) 023509.
- [36] T. Padmanabhan, Phys. Rev. D **66** (2002) 021301.
- [37] A. Feinstein, Phys. Rev. D **66** (2002) 063511.
- [38] A. R. Liddle, Phys. Rev. D **68** (2003) 103504.
- [39] A. R. Liddle, P. Parsons and J. D. Barrow, Phys. Rev. D **50** (1994) 7222.
- [40] J. E. Lidsey, A. R. Liddle, E. W. Kolb, E. J. Copeland, T. Barreiro and M. Abney, Rev. Mod. Phys. **69** (1997) 373.
- [41] S. Dodelson, L. Hui, “A horizon ratio bound for inflationary fluctuations”, [arXiv:astro-ph/0305113].
- [42] A. R. Liddle and S. M. Leach, “How long before the end of inflation were observable perturbations produced?”, [arXiv:astro-ph/0305263].
- [43] J. Garriga, V. F. Mukhanov, Phys. Lett. B **458** (1999) 219-225.
- [44] J. c. Hwang and H. Noh, Phys. Rev. D **66** (2002) 084009.
- [45] V. F. Mukhanov, H. A. Feldman, and R. H. Brandenberger, Phys. Rep. **215** (1992) 203.
- [46] Y. S. Song and L. Knox, Phys.Rev. D **68** (2003) 043518.
- [47] N. Kaloper, M. Kleban, A. E. Lawrence and S. Shenker, Phys. Rev. D **66** (2002) 123510; N. Bartolo, S. Matarrese and A. Riotto, Phys. Rev. D **64** (2001) 123504; D. Wands, N. Bartolo, S. Matarrese and A. Riotto, Phys. Rev. D **66** (2002) 043520; L. Hui, W. H. Kinney, Phys. Rev. **D65** (2002) 103507.
- [48] D. H. Lyth and A. Riotto, Phys. Rept. 314 (1999) 1.
- [49] A. A. Gerasimov and S. L. Shatashvili, JHEP 0010 (2000) 034; D. Kutasov, M. Marino and G. W. Moore, JHEP 0010 (2000) 045.
- [50] A. Sen, Mod. Phys. Lett. A **17** (2002) 1797.
- [51] L. R. W. Abramo, F. Finelli, “Cosmological dynamics of the tachyon with an inverse power-law potential”, [arXiv:astro-ph/0307208].

- [52] S. M. Leach and A. R. Liddle, “Constraining slow-roll inflation with WMAP and 2dF”, [arXiv:astro-ph/0306305].
- [53] H. Kodama, M. Sasaki, Prog. Theor. Phys. Suppl **78**, (1984).
- [54] J. García-Bellido and D. Wands, Phys. Rev. D**53** (1996) 5437.